

MOLECULAR MODELING OF CRACKS AT INTERFACES IN NANOCERAMIC COMPOSITES

F. Pavia^{a*}, W. A. Curtin^a

^a*Institute, of Mechanical Engineering, EPFL, Lausanne, Switzerland*
**fabio.pavia@epfl.ch*

Keywords: molecular modeling, crack deflection, toughness, nanotube ceramic matrix composites

Abstract

Toughness in Ceramic Matrix Composites (CMCs) is achieved if crack deflection can occur at the fiber/matrix interface, preventing crack penetration into the fiber and enabling energy-dissipating fiber pullout. To investigate toughening in nanoscale CMCs, atomistic models are used to study how matrix cracks behave as a function of the degree of interfacial bonding/sliding, controlled by the density of C interstitial atoms, at the interface between carbon nanotubes (CNTs) and a diamond matrix. In our simulations incident matrix cracks do not penetrate into the nanotube. Under increased loading, weaker interfaces fail in shear while stronger interfaces do not fail and, instead, the CNT fails once the stress on the CNT reaches its tensile strength. Interface deflection versus fiber penetration is found to depend on the relative bond strengths of the interface and the CNT, with CNT failure occurring well below the prediction of the toughness-based continuum He-Hutchinson model.

1. Introduction

The outstanding mechanical properties of nanofibers, and in particular carbon nanotubes (CNTs), make them good candidates as reinforcements for ceramic matrix nano-composites (CMnC) or hybrid/hierarchical composites for a variety of applications in the sector of the aerospace. The full capabilities of nanoceramic composites are not fully realized, however, since the desirable macroscopic performance depends on the operation of nanoscale deformation and fracture mechanisms and the effects of the actual nanostructure [1,2,3,4].

Theoretical and numerical investigations of nanotube reinforced ceramic matrices have thus been used to identify key nanoscale deformation features and their dependence on CNT and interface properties. The prior works studied pullout problems with relatively uniform sliding along a short length of interface, and so do not address the crucial issue of matrix cracks impinging on the interface and nanofiber. As a matrix crack approaches a fiber, the crack can either deflect along the interface (leading to toughening by other mechanisms) or penetrate into the fiber (leading to brittle behavior), depending on the relative toughness and strength of the interface and fiber, respectively. If the interface is too tough, debonding does not occur [5] and the reinforcing fibers eventually break near the matrix crack plane, resulting in low fracture toughness. Whether these continuum analyses, especially those of He and Hutchinson [6,7], are applicable at the nanoscale and, moreover, for CNTs that are only a few atom layers in thickness, is not known. Our goal here is thus to use direct atomistic models to probe these fracture processes, with systematic control of the degree of interfacial bonding and sliding.

2. Molecular Models of Cracked Nanoceramic Composites

We study a crack propagating in a diamond matrix and impinging at the interface of single-wall CNTs (SWCNTs) and double-wall CNTs (DWCNTs), with interstitial carbon atoms coupling matrix and nanotube. Figures 1 a-b show a general picture of the simulation unit cell used here. SWCNTs and DWCNTs are generated in ideal armchair configurations with a C-C bond length of 1.42 Å and an outer wall radius of $r_o=8.2$ Å. The DWCNTs have interwall bonding to mechanically couple them and increase the overall load capacity of the nanotube through load transfer from the outer to the inner walls. Here we use sp^3 bonds between pairs of nearby carbon atoms at random locations in the two walls with a density of 3%, which allows load transfer over a distance of approximately 14Å [8]. The matrix is diamond with a C-C bond length of 1.54 Å and oriented with the [111] direction parallel to CNT axis. Overall cross-sectional dimensions of 40 Å × 39 Å and height 1200 Å are used, with a total cross-section of the composite of approximately 15.8 nm² and with periodic boundary conditions in the lateral dimensions. The radius r of the hole in the diamond matrix is such that the initial bond lengths between carbon interstitials in the interface and carbon atoms in both the matrix and the CNT have, on average, values close to the nominal diamond C-C bond length.

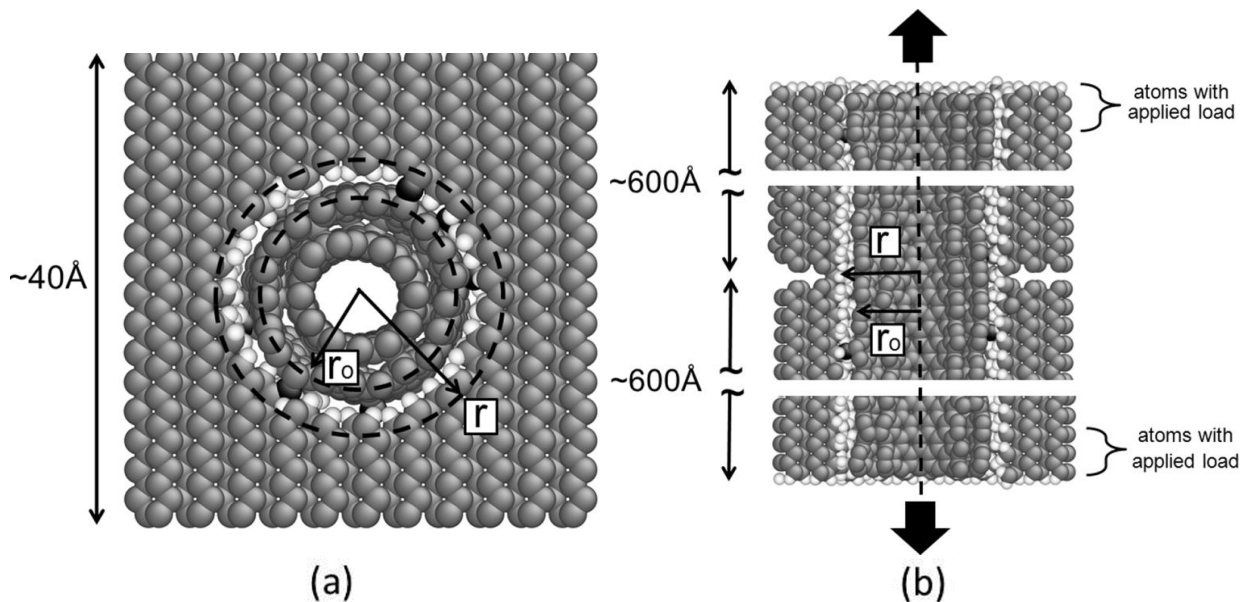


Figure 1. (a) Top view and (b) side view of an atomistic model of a nanocomposite unit cell composed of a diamond carbon matrix and a DWCNT. Carbon atoms in the matrix and nanotube are gray, random interstitial carbon atoms in the interface are black, and hydrogen atoms are white. In (b) an annular crack is inserted by removing the carbon atoms at the center of the matrix. During loading in direction of the tube axis, increments of displacement or force are applied to the carbon atoms at the boundary of the composite cell, subfigure (b).

As chemical vapor deposition and infiltration processes are commonly used to make carbon/carbon nanocomposite materials, we expect the interface between matrix and nanotube to be hydrogen saturated, with some carbon interstitial atoms linking matrix and nanotube. In our molecular model interstitial carbon atoms are placed at random positions between the diamond matrix and CNT to capture this realistic interface state and to control interface adhesion and friction. The remaining unsaturated bonds on the interface are saturated with hydrogen atoms. Following Pavia and Curtin [3], we take the interface radius as in between the outer CNT wall and the innermost diamond matrix atoms, and we define an interface interstitial density as $\rho=n/A$, where n is the number of interstitials and A is the nominal area of

interface. We have shown that the frictional sliding resistance τ_0 , the interface strength τ_s , and the shear modulus of the interface μ_i , scale with the density of interstitial atoms as [3]

$$\tau_0 \approx 3\rho \text{ GPa}\cdot\text{nm}^2 \quad ; \quad \tau_s \approx 6\rho \text{ GPa}\cdot\text{nm}^2 \quad ; \quad \mu_i \approx 4.6\rho \text{ GPa}\cdot\text{nm}^2 \quad (1)$$

Here, we use $\rho = 0.13 - 1.5 \text{ nm}^{-2}$ corresponding to interface frictional stresses τ_0 between 400 MPa and 4.5 GPa, strengths τ_s between 800 MPa and 9 GPa, and interface shear moduli μ_i between 600 MPa and 7 GPa.

We then introduce an initial crack into the diamond matrix by removing matrix C atoms along the midplane of the specimen at a distance greater than 13 \AA from the axis of the CNT, as shown in Figure 1b. Axially loading of the composite then drives crack growth and its impingement on the interface with the CNT. In addition to explicit matrix crack simulations, we also perform “pullout simulations” wherein the matrix crack initially extends to the interface, i.e. the entire matrix is cracked, and load is applied starting from zero.

3. Crack Impingement in Diamond Nano-Composites

After the diamond matrix fractures, the crack faces open, the nanotube is stretched, and the interface is sheared (see Figure 2). We measure the crack opening 2δ and the force F_{pull} and stress T on the nanotube at the crack plane.

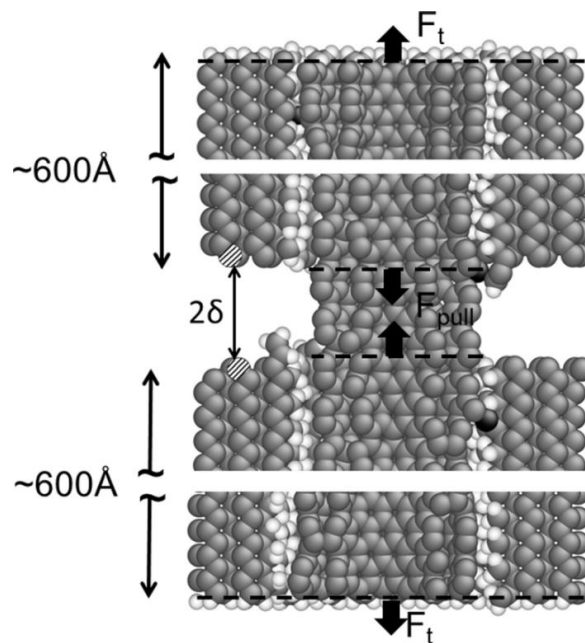


Figure 2. View of the zone where the nanotube is bridging the crack faces after the diamond matrix breaks and opens in axial direction. The density of interstitials is $\rho=0.53 \text{ nm}^{-2}$. The bonds with the interstitial atoms are distorted by shear deformations while the nanotube is stretched between the opening crack surfaces. The force pulling the nanotube and the total force held by the composite equilibrate with $F_{pull} = F_t$. The crack opening 2δ is computed from the displacements of the two hatched C atoms on the upper and lower crack faces.

Figure 3 shows the measured stress T versus the crack half-opening δ for different interstitial atoms densities. The stress and crack opening are normalized by the nanotube strength σ_s and hole radius r , respectively. Under force-control, just after crack propagation, stresses of $T=36$ and 38 GPa are imposed on the SWCNTs and DWCNTs, respectively, corresponding to approximately $T/\sigma_s \approx 0.8$. The SWCNTs fail immediately at stresses below their nominal

strength, while the DWCNTs do not. Under displacement control, the matrix crack makes the system more compliant and so forces on the CNTs are reduced and neither SWCNTs nor DWCNTs fail immediately at crack propagation and the system can sustain additional loading. The *in-situ* strength of the CNT can be influenced by the interstitial C atoms, or more generally by the creation of “functionalization” or bonding between CNTs and a matrix material. After crack impingement, the interstitial carbon atoms can locally tear open the outer shell by inducing the failure of a bond between two adjacent carbon atoms, causing SWCNT to break at a peak stress approximately 20% lower than the effective strength of the pristine SWCNT. On the contrary, DWCNTs are relatively insensitive to these defects because the sp^3 interwall bonds restrain the propagation of the defects nucleated on the external shell.

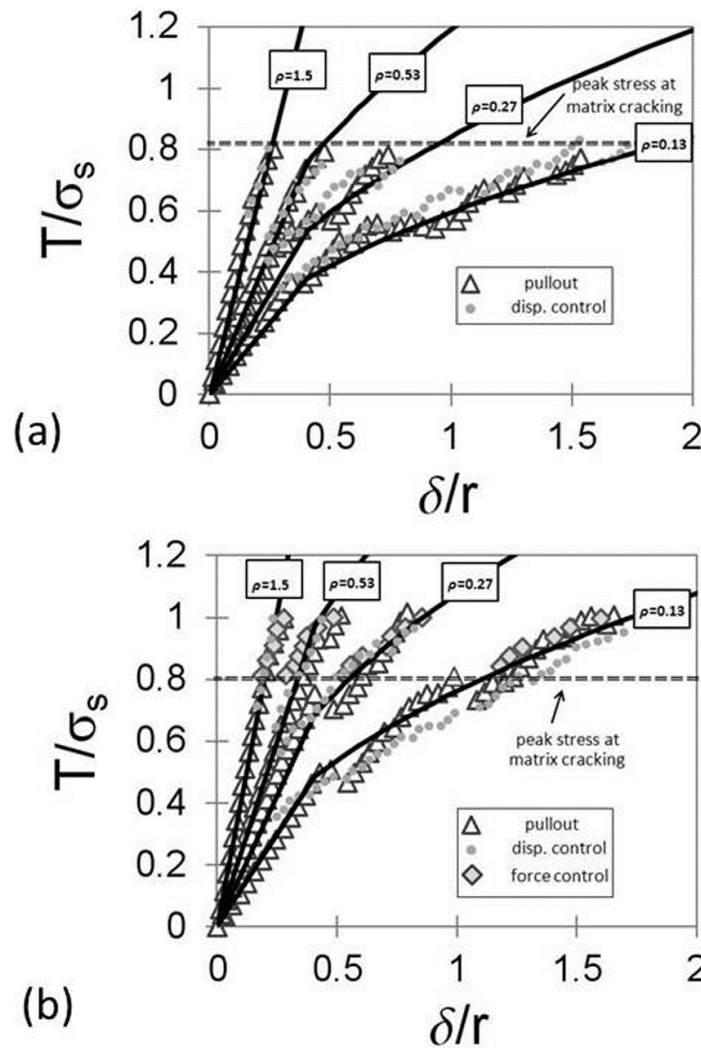


Figure 3. Peak stress T as a function of the crack half-opening δ for increasing values of interstitials density at the interface for (a) SWCNTs and (b) DWCNTs. The nanotube strength, σ_s , of 44 GPa for SWCNTs and of 47 GPa for DWCNTs, and the radius of the hole in the diamond matrix, $r=11.2 \text{ \AA}$, are used to normalize the values of stress and crack opening. Crack impingement simulations under force or displacement applied to the composite cell are shown respectively by diamond and filled circular markers and collapse on the curves obtained for nanotube pullout directly from the cracked surfaces, shown by triangular markers. Also show (lines) are the predictions of the shear lag model for each density of interstitials.

Figure 3 also shows the results from our “pullout” simulations where the crack starts at the interface. The pullout simulations are essentially identical to the displacement-controlled

loading cases after matrix cracking, which demonstrates that there are no effects due to the dynamics of the crack propagation up to the interface that influence the subsequent debonding, sliding, and fracture behavior. Differences between the simulations shown in Figure 3 are due to different random distributions of interstitials at the interface. The predictions of an analytic shear-lag model following the work of [5,14], with all material parameters specific to the systems used and thus using no adjustable parameters, are also shown in Figure 3. For the entire range of interstitial densities ρ considered in this work, the shear-lag model very accurately predicts the results of the molecular simulations in considerable detail. Of particular note is the point of debonding, controlled by the interfacial shear strength, and the curvature in the displacement during the subsequent sliding regime, controlled by the interface friction stress.

The simulations show a transition to “brittle” behavior, i.e. fiber fracture rather than interface debonding, at an interstitial density of 0.53 nm^{-2} , corresponding to an interface strength of 3.2 GPa. The He-Hutchinson model [6,7] posits that the debonding/fiber-fracture depends on the ratio of the fracture toughness of the interface and fiber, Γ_i and Γ_f , respectively. Although here both matrix and nanotube are inherently anisotropic, with very high axial moduli and very low shear moduli, they have comparable values for the elastic properties. In this case, the He-Hutchinson analysis predicts interface debonding for ratios of interface to fiber toughness lower than $\Gamma_i/\Gamma_f \approx 0.25$; this ratio would increase for different elastic properties as a function of the Dundurs’ parameters [9]. To assess the validity of the He-Hutchinson analysis, we calculate from the molecular simulations as discussed in [11] the interfacial energy Γ_i between matrix and nanotube as a function of the interstitials density and the nanotube fracture energy Γ_f and obtain a ratio relevant to the He-Hutchinson model $\Gamma_i/\Gamma_f \approx 0.004\text{-}0.0425$, far below the He-Hutchinson critical value of 0.25, implying that all the interfaces studied here should debond, in contrast to our observation of CNT failure at the higher interstitial densities. The He-Hutchinson criterion thus fails in direct application to CNT nanoceramic composites.

The He-Hutchinson model is an energy-criteria based on the analysis of the stress concentration factor ahead of a crack that advances infinitesimally into the interface or fiber. The applicability of a continuum stress intensity factor for a multiwall nanotube “fiber” of only a few atoms in thickness and for interface bonding generated by discrete interstitials C atoms is questionable. Moreover, as discussed by Parmigiani and Thouless [10], for a very weak interface and a tough reinforcement, the crack path selection is controlled only by the ratio between the interface strength and the fiber strength, and a stress-intensity/energy-based fracture criterion fails. Our results are qualitatively consistent with the results of Parmigiani and Thouless, as follows. We find a transition from “debonding” to “penetration”, or “brittle” behavior, for an interface strength of approximately 3.2 GPa, with nanotube effective strengths between 44 and 47 GPa, leading to a critical strength ratio of ~ 14 . This value is greater than the asymptotic value of 3.2 shown in the work of Parmigiani and Thouless. However, they show that the ratio of the interface fracture length scale $E_m\Gamma_i/\tau_s$ to the film thickness h influences the transition between penetration and deflection, with increasing $E_m\Gamma_i/h\tau_s$ shifting the critical stress ratio to higher values. In our system, we take h to be the matrix thickness and can then estimate $E_m\Gamma_i/h\tau_s \approx 20$. For $E_m\Gamma_i/h\tau_s \approx 10$, Parmigiani and Thouless show a critical strength ratio of 8, which is larger than 3.2 and is approaching our observed value of ~ 14 . Given differences in geometry (thick matrix on thin nanotube vs. thin film on a semi-infinite substrate), and the absence of results in Parmigiani and Thouless for values larger than $E_m\Gamma_i/h\tau_s \approx 10$, we can consider our present results to be qualitatively consistent with Parmigiani and Thouless.

The concept of a critical stress intensity factor does reflect the existence of an atomic material bond strength and suggests the use of a bond strength criterion for determining debonding versus penetration: if the stress on the interface bonds reaches their strength before the stress on the CNT bonds reach their strength, then debonding will occur. Conversely, CNT fracture will occur if the CNT bonds reach their strength first. We can estimate the transition point based on these atomic bond strengths and independent of ratio of the nanotube to interface toughness using a shear lag model analysis as discussed in [11]. The stress on the CNTs can be well-estimated by assuming that all walls carry equal load. The CNT stress in the plane of the matrix crack is then σ_{app}/f and the CNTs will fail if $\sigma_{app}/f=\sigma_s$, hence at a value of applied stress $\sigma_{app}=f\sigma_s$. The transition from debonding to CNT failure is then obtained when interfacial debonding commences at an applied load causing the the nanotube to fail, which occurs at an interfacial strength given by

$$\tau_s = \sigma_s \sqrt{\frac{\mu E_m (1-f)}{2E_c E_f \log(r_m/r)}}, \quad (2)$$

where μ is the shear modulus of the composite unit cell, σ_s is the strength of the reinforcement, f is volume fraction of reinforcement, E_m is the elastic modulus of the matrix, E_f is the effective elastic modulus of the nanotube, E_c is the elastic modulus of the composite, r_m is the radius of the matrix where the axial matrix stress is assumed to be concentrated, and r is the radius of the hole in the carbon matrix. Since the relatively loosely-bound interface interstitial atoms have a low effective shear modulus, we have shown in [11] that

$$\mu \approx \mu_i \frac{\log(r_m/r)}{\log(r/r_o)}, \quad (3)$$

where μ_i is the shear modulus of the interface between nanotube and matrix and r_o is the radius outer wall of the nanotube. Both μ_i and τ_s depend on the density of interstitials through Eq.1, so we can write $\mu_i = 0.77\tau_s$, substitute into Eq.2, and solve for the critical value of interface strength above which the composite will become embrittled by failure of the nanotube as

$$\tau_s \geq \frac{(1-f)E_m \sigma_s^2}{2.61E_f E_c \log(r/r_o)}. \quad (4)$$

For the simulated nanocomposites, Eq.4 yields $\tau_s = 3.4$ GPa and 3.6 GPa for DWCNTs and SWCNTs respectively, using the effective nanofiber strength, corresponding to an interfacial interstitial density $\rho = 0.57-0.6$ nm⁻² using Eqs.1. Our simulations show that CNT failure with no debonding occurs for $\rho = 1.5$ nm⁻² and that debonding does occur for $\rho = 0.53$ nm⁻², just below the value predicted by Eq.4. This stress-based embrittlement criterion is thus in quantitative agreement with our simulations.

We would expect the concept of a continuum stress intensity factor to be valid in MWCNTs with increasing number of walls and sufficient interwall coupling but it is difficult to be quantitative. In any case, the transition given by Eq.2 should be an upper limit, since we assume that all the walls in the nanotube are equally stressed in the plane of the matrix crack; any stress concentration that increases the stress on the outer nanotube wall would drive brittle fracture at lower interfacial strengths. In the usual assumption that all elastic moduli in

the CMC are similar in magnitude, Eq.2 would suggest that the transition to brittle behavior would require very strong interfaces,

$$\tau_s \approx \sigma_s \sqrt{\frac{1-f}{2\log(r_m/r)}}, \quad (5)$$

i.e. comparable to the fiber strength itself. However, our analysis shows that if the interface in a nanocomposite is controlled by a moderate density of functionalizing elements (interstitial C atoms), then the effective shear modulus can be comparable to the shear modulus of the interface, which is much lower than the moduli of the matrix or the fiber. Thus, for moderate functionalization, Eq.4 applies, which we can write approximately, i.e. neglecting numerical factors of order unity, as

$$\tau_s \approx \sigma_s \left(\frac{\sigma_s}{E_f} \right) \approx \sigma_s \varepsilon_{fs}, \quad (6)$$

Where ε_{fs} is the failure strain of the nanofiber. Since $\varepsilon_{fs} \ll 1$, the critical interface strength must be much smaller than the nanofiber strength. Therefore, although much of the mechanics is similar, the design of nanoscale composite interfaces is fundamentally different than that at the micron scale in one important respect. Specifically, the brittle/ductile transition occurs at much lower interface strengths, relative to the intrinsic fiber strength, and this implies that the density of functionalized interfaces must be quite low. For a nanoscale composite interface there is a significant decrease in the brittle/ductile transition point for interfacial strength with respect to microscale interfaces. The details depend on the nature of the functionalizing bonds (strength and stiffness), with the results here for C interstitials, which can form strong and stiff bonds with both the diamond matrix and the graphitic CNTs, presumably providing an upper limit to the achievable interface bond properties.

4. Summary

We have simulated an annular crack propagating through a diamond matrix and impinging on the interface with single-wall and double-wall defect-free nanotubes to understand the response of the nanofiber and interface to the matrix crack impingement as a function of interface strength and sliding resistance. Crack impingement is investigated as a function of the degree of bonding between matrix and nanotube. Even for the strongest interfaces studied here (9 GPa shear strength), incident matrix cracks do not penetrate into the nanotube, even if they are not deflected along the interface. Under increased loading, “weak” interfaces fail in shear followed by interfacial sliding, leading to “tough” materials. “Strong” interfaces do not debond, and instead the CNT fails, leading to a “brittle” low-toughness material. In both cases, the entire response is accurately captured by a shear-lag model. The transition between “weak” and “strong” interfaces, and hence “tough” and “brittle” composite behavior, is not governed by the interface and nanofiber fracture energies, as predicted by the He-Hutchinson analysis. Rather, the transition is determined by their fracture strengths (interface shear strength and nanofiber tensile strength). For the systems studied here, brittle behavior is found well below the conditions predicted by the He-Hutchinson energy criterion, but in excellent agreement with the strength criterion evaluated using a shear-lag model. The transition to brittle behavior occurs at much lower levels of interface functionalization (here, interstitial C atoms) than would be anticipated by the continuum models, due to the low shear modulus of low levels of functionalization; this alters the interface design criterion for nanocomposites.

The CNT strengths themselves are influenced by the “functionalization” at the interface, which facilitate formation of small-scale defects that can cause fracture in SWCNTs near the matrix crack. MWCNTs with internal coupling between walls are less sensitive to such defects. With higher load-carrying capacity due to the extra walls and the interwall coupling, MWCNTs are thus advantageous, as concluded in examining other nanocomposite properties [12,13]. Overall, our results provide directions for obtaining toughening in CNT-based nanoCeramic Matrix Composites through the use of both interwall-coupled MWCNT-reinforced ceramics and a controlled, and relatively low, degree of functionalization of the outer walls to the surrounding matrix.

References

- [1] K. Ahmad, W. Pan. Hybrid nanocomposites: A new route towards tougher alumina ceramics. *Compos. Sci. Technol.* 68(6):1321–1327, 2008.
- [2] W. A. Curtin, B. W. Sheldon. CNT – reinforced ceramics and metals. *Mater. Today* 11: 44-49, 2004.
- [3] F. Pavia, W. A. Curtin. Interfacial sliding in carbon nanotube / diamond matrix composites. *Acta Mater.* 59(17): 6700–6709, 2011.
- [4] E. T. Thonstenson, W. Z. Li, D. Z. Wang, Z. F. Ren, T. W. Chou. Carbon nanotube/carbon fiber hybrid multiscale composites. *J. Appl. Phys.* 91(9): 6034–6037, 2002.
- [5] B. Budiansky, J. W. Hutchinson, A. G. Evans. Matrix fracture in fiber – reinforced ceramics. *J. Mech. Phys. Solids* 34(2): 167–189, 1986.
- [6] M. Y. He, J. W. Hutchinson. Crack deflection at an interface between dissimilar elastic materials. *Int. J. Solids Struct.* 25(9): 1053–1067, 1989.
- [7] M. Y. He, A. G. Evans, J. W. Hutchinson. Crack deflection at an interface between dissimilar elastic materials: role of residual stresses. *Int. J. Solids Struct.* 31(24): 3443–3455, 1994.
- [8] E. M. Byrne, A. Letertre, M. A. McCarthy, W. A. Curtin, Z. H. Xia. Optimizing load transfer in multiwall nanotubes through interwall coupling: theory and simulation. *Acta Mater.* 58(19): 6324–6333, 2010.
- [9] J. Dundurs. Discussion: Edge-bonded dissimilar orthogonal elastic wedges under normal and shear loading. *J. Appl. Mech.* 36(3): 650–652, 1969.
- [10] J. P. Parmigiani, M. D. Thouless. The roles of toughness and cohesive strength on crack deflection at interfaces. *J. Mech. Phys. Solids* 54(2): 266–287, 2006.
- [11] F. Pavia, W. A. Curtin. Molecular modeling of cracks at interfaces in nanoceramic composites. *J. Mech. Phys. Solids* 61 (10): 1971–1982, 2013.
- [12] E. M. Byrne, M. A. McCarthy, Z. H. Xia, W. A. Curtin. Multiwall nanotubes can be stronger than single wall nanotubes and implications for nanocomposites design. *Phys. Rev. Lett.* 103(4): 045502, 2009.
- [13] Z. H. Xia, P. Guduru, W. A. Curtin. 2007. Enhancing mechanical properties of multiwall carbon nanotubes via sp^3 interwall bridging. *Phys. Rev. Lett.* 98(24): 245501, 2007.
- [14] M. Sutcu, W. B. Hillig. The effect of fiber-matrix debond energy on the matrix cracking strength and the debond shear strength. *Acta Metall. Mater.* 38(12): 2653–2662, 1990.